

Nonlinear growth acceleration in gyrofluid simulations of collisionless reconnection

A. Biancalani,* B. D. Scott

Max-Planck-Institut für Plasmaphysik, Euratom Association, D-85748 Garching, Germany

Introduction

Magnetic reconnection is an instability which occurs in magnetized plasmas, associated to a breaking and reconnecting of the magnetic field lines [1]. Characteristic resistive times are too large in many situations, like for instance in hot plasmas, where the resistivity is low. In these situations, collisionless reconnection, due to finite inertia of the electrons, can provide faster reconnection rates than resistive reconnection [2, 3]. In many cases the ion Larmor radius is larger than the reconnective inertial layer and 3 dimensional nonlinear phenomena can develop. In this paper we want to face these cases, therefore we adopt a 3D gyro-fluid model.

Two dimensional studies with a gyrofluid model were performed in Ref. [4] with gyrofluid code REC2, in periodic configuration, with flat temperature and density profiles. Finite Larmor radius effects (FLR) were investigated with REC2 in Ref. [5] and more recently in Ref. [6]: linear growth rates were found consistent with analytical scaling with ρ_i . Three dimensional studies were performed with a two-fluid model in Ref. [7], in the large Δ' regime. It was found that small perpendicular scales develop in proximity of the island separatrix [8, 9]. Nonlinear acceleration has been found at the beginning of the nonlinear phase in Ref. [10]. The value of the nonlinear growth rate was found to increase for smaller values of ρ_s/L and d_e/L . The nonlinear growth rate was found at values up to twice the linear growth rate.

In this paper, we investigate the small Δ' regime, and push the limit of very small values of ρ_s/L and d_e/L , for values of β in the transition between fusion and space plasmas.

Model equations.

Reconnecting modes are investigated, evolving in a three dimensional Harris-pinch configuration ($B_y(x) = \hat{B}_y \tanh(x)$, $B_z = \text{const.}$). Flat density and temperature profiles are initialized.

A 3D gyrofluid code named GEM (Gyrofluid ElectroMagnetic) is used for our numerical simulations [11]. A strong guide fields is assumed and fast magneto-sonic waves are neglected. Frequencies lower than the ion gyro-frequency are considered. The gyrofluid model equations

*also at Max-Planck-Institut für Sonnensystemforschung, Katlenburg-Lindau, Germany

for the ions are:

$$\left(\frac{\partial}{\partial t} + \mathbf{u}_E \cdot \nabla\right) \tilde{n}_i = -B \nabla_{\parallel} \frac{\tilde{u}_{\parallel}}{B} \quad (1)$$

$$\hat{\beta} \frac{\partial \tilde{A}_{\parallel}}{\partial t} + \hat{\varepsilon} \left(\frac{\partial}{\partial t} + \mathbf{u}_E \cdot \nabla\right) \tilde{u}_{\parallel} = -\nabla_{\parallel} (\tilde{\phi}_G + \tau_i \tilde{n}_i) \quad (2)$$

and for the electrons:

$$\left(\frac{\partial}{\partial t} + \mathbf{v}_E \cdot \nabla\right) \tilde{n}_e = -B \nabla_{\parallel} \frac{\tilde{v}_{\parallel}}{B} \quad (3)$$

$$\hat{\beta} \frac{\partial \tilde{A}_{\parallel}}{\partial t} - \hat{\mu} \left(\frac{\partial}{\partial t} + \mathbf{v}_E \cdot \nabla\right) \tilde{v}_{\parallel} = -\nabla_{\parallel} (\tilde{\phi} - \tilde{n}_e) \quad (4)$$

where the tilde symbol denotes perturbed quantities, $\tau_i = T_i/T_e$, n , u and v are the fluid density and ion and electron velocities, and ϕ and A are the scalar and vector potentials. The parameters $\hat{\beta}$, $\hat{\varepsilon}$ and $\hat{\mu}$ are defined by: $\hat{\beta} = \beta_e \hat{\varepsilon}$, $\hat{\varepsilon} = (qR/L)^2$ and $\hat{\mu} = \mu_e \hat{\varepsilon} = (m_e/m_i) \hat{\varepsilon}$, where $\beta_e = 4\pi p_e/B^2$, and qR and L are the scale length along and perpendicular to the equilibrium magnetic field.

Note that all quantities with symbol $\hat{\cdot}$ are normalized to $\hat{\varepsilon}$. The parallel gradient is calculated in the direction parallel to the total (equilibrium plus perturbed) magnetic field, and the gyro-averaged scalar potential is defined as $\tilde{\phi}_G = \Gamma_0^{1/2}(\tilde{\phi})$. The advection velocities v_E and u_E are the $E \times B$ drifts, given by $c \nabla \tilde{\phi}_G \times B/B^2$ (where for the electrons $\tilde{\phi}_G = \tilde{\phi}$).

Moreover, the polarization and induction equations are:

$$\Gamma_0^{1/2} \tilde{n}_i + \frac{\Gamma_0 - 1}{\tau_i} \tilde{\phi} = \tilde{n}_e, \quad -\nabla_{\perp}^2 \tilde{A}_{\parallel} = \tilde{J}_{\parallel} = \tilde{u}_{\parallel} - \tilde{v}_{\parallel}$$

We also use the Padé approximant forms: $\Gamma_0 = (1 - \rho_i^2 \nabla_{\perp}^2)^{-1}$, $\Gamma_0^{1/2} = (1 - \rho_i^2 \nabla_{\perp}^2/2)^{-1}$, where ρ_i is the ion gyro-radius.

We consider a plasma regime with $\Delta' \rho_s = 0.7$. We obtain a very thin reconnection layer with respect of the perpendicular size of the simulation box ($\rho_s/L_x = 0.008$). A deuterium plasma is considered ($\mu_e = 0.00027$) in our simulations. The ion to electron temperature ratio is considered unitary, $\tau_i = 1$, unless otherwise specified.

A gyro-fluid model is capable of investigating finite Larmor radius effects on the reconnection dynamics. The linear growth rate γ_L , is shown to increase with the ion Larmor radius via the

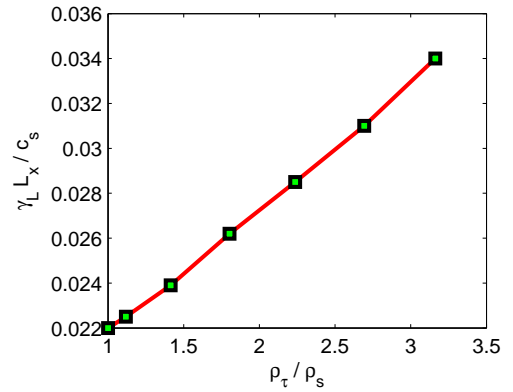


Figure 1: Linear growth rate, normalized to the sound speed, versus the gyro-radius to sound gyro-radius average ρ_{τ} , for $\Delta' \rho_s = 0.7$, $\beta_e = 5.4 \cdot 10^{-5}$.

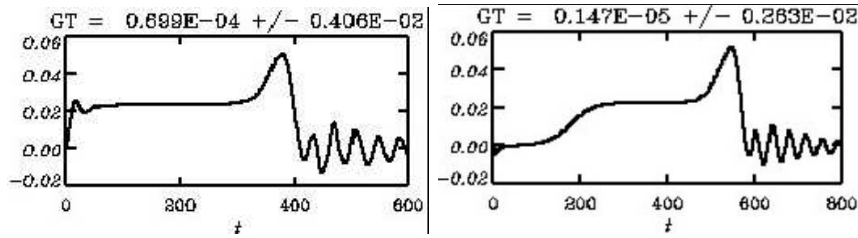


Figure 2: Evolution of the growth rates for the run starting with a magnetic island seed (left), and with a white noise (right). The nonlinear acceleration is found in the phase $t=350-400 L/c_s$ for the case with initial seed, and at $t=500-550 L/c_s$ for the case with initial white noise.

quantity ρ_τ , where $\rho_\tau = \sqrt{\rho_i^2 + \rho_s^2}$ (see Fig. 1). This is consistent with the analytical theoretical prediction given in Ref. [3]. No qualitative changes are found in the dynamics of our interest due to finite larmor radius effects, neither in the linear nor in the nonlinear phase.

Nonlinear evolution.

We perform two kinds of runs: one starting with an island seed and one starting with an initial white noise. In both the cases, after a transient phase the growth becomes exponential in time, and the growth rate tends to a constant value.

This phase where the growth rate is constant in time is named linear phase. At the beginning of the nonlinear phase, we have an acceleration of the reconnection growth, associated with a peak in the growth rate (see Fig. 2).

The ratio between nonlinear and linear growth rates increases with increasing beta, reaching values up to more than one order of magnitude at β_e of the order of $10^{-3}-10^{-2}$. For our normalization convention (all quantities are normalized to ρ_s) increasing β_e corresponds in keeping constant d_e and increase all other length scales. After the nonlinear acceleration we find a saturation of the island, due

to smaller structures forming inside the magnetic island and to secondary instabilities of the Kelvin-Helmoltz type, forming at the separatrix. For the whole runs the energy conservation is accurately checked. In fact, the contribution of the sub-grid dissipation is always calculated and

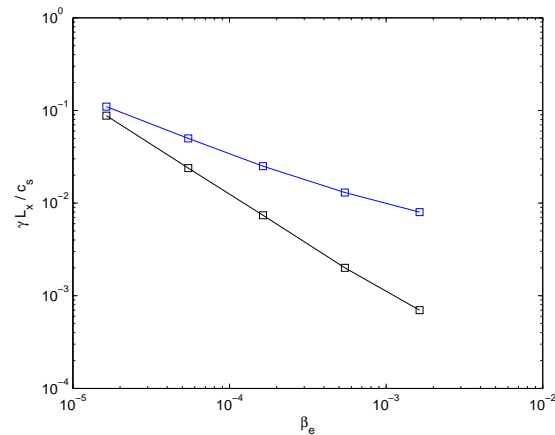


Figure 3: Growth rates vs beta. Nonlinear growth rates are in blue; linear growth rates in black. Note that for β_e of the order of $10^{-3}-10^{-2}$, the nonlinear growth rate is one order of magnitude higher than the linear growth rate.

checked to be negative: this gives us the certainty that reconnection is physical and is not driven by artificial effects.

Acceleration in collisionless reconnection growth rates were studied in literature in Ref. [10] and found to be linked to the presence of narrow current layers. Also, in resistive reconnection nonlinear acceleration was found to be associated with turbulence forming around the X-point (see e.g. Ref. [12]). In our simulations, the novel result is that the nonlinear acceleration is reaching values one order of magnitude higher than the linear growth rates, assuming the form of explosive reconnection. Current singularities are confirmed to be present at the separatrix during the nonlinear phase of reconnection. The study of their size and importance in the reconnection dynamics is still in progress.

Acknowledgments

This work was carried out in a collaboration with the Max-Planck institute for solar system research at Katlenburg-Lindau, Germany. The authors thank Francesco Pegoraro, Francesco Califano, Daniele Del Sarto and Tiago Ribeiro for enlightening discussions.

References

- [1] H.P. Furth, J. Killeen and M.N. Rosenbluth, *Phys. Fluids* **6**, 459 (1963)
- [2] A.W. Edwards *et al.*, *Phys. Rev. Lett.* **57**, 210 (1986)
- [3] F. Porcelli, *Phys. Rev. Lett.* **66**, 425 (1991)
- [4] B.D. Scott and F. Porcelli, *Phys. Plasmas* **11**(12), 5468 (2004)
- [5] A. Biancalani and B.D. Scott, 37th EPS Conf. on Plasma Physics (Dublin, Ireland, 21-25 June 2010) Paper P4.108 <http://ocs.ciemat.es/EPS2010PAP/pdf/P4.108.pdf>
- [6] D. Grasso, E. Tassi and F.L. Waelbroeck, *Phys. Plasmas* **17**, 082312 (2010)
- [7] D. Borgogno, D. Grasso, F. Porcelli, F. Califano, F. Pegoraro and D. Farina, *Phys. Plasmas* **12**, 032309 (2005)
- [8] M. Ottaviani and F. Porcelli, *Phys. Rev. Lett.* **71**, 3802 (1993)
- [9] D. Grasso, F. Califano, F. Pegoraro and F. Porcelli, *Phys. Rev. Lett.* **86**(22), 5051 (2001)
- [10] A. Bhattacharjee, K. Germaschewski, and C. S. Ng, *Phys. Plasmas* **12**, 042305 (2005)
- [11] B.D. Scott, *Pl. Phys. Control. Fus.* **45**, A385 (2003)
- [12] N.F. Loureiro *et al.*, *Mon. Not. R. Astron. Soc.* **399**, L146 (2009)